



**HAL**  
open science

## Flowable Electrodes from Colloidal Suspensions of Thin Multiwall Carbon Nanotubes

Massinissa Hamouma, Wilfrid Neri, Xavier Bril, Jinkai Yuan, Annie Colin,  
Nicolas Brémond, Philippe Poulin

► **To cite this version:**

Massinissa Hamouma, Wilfrid Neri, Xavier Bril, Jinkai Yuan, Annie Colin, et al.. Flowable Electrodes from Colloidal Suspensions of Thin Multiwall Carbon Nanotubes. *Colloids and Interfaces*, 2024, 8 (3), pp.32. 10.3390/colloids8030032 . hal-04744950

**HAL Id: hal-04744950**

**<https://hal.science/hal-04744950v1>**

Submitted on 19 Oct 2024

**HAL** is a multi-disciplinary open access archive for the deposit and dissemination of scientific research documents, whether they are published or not. The documents may come from teaching and research institutions in France or abroad, or from public or private research centers.

L'archive ouverte pluridisciplinaire **HAL**, est destinée au dépôt et à la diffusion de documents scientifiques de niveau recherche, publiés ou non, émanant des établissements d'enseignement et de recherche français ou étrangers, des laboratoires publics ou privés.

---

# Flowable electrodes from colloidal suspensions of thin multi-wall carbon nanotubes

Massinissa Hamouma<sup>1</sup>, Wilfrid Neri<sup>1</sup>, Xavier Brill<sup>1</sup>, Jinkai Yuan<sup>1,2</sup>, Annie Colin<sup>4</sup>, Nicolas Brémond<sup>3</sup>, Philippe Poulin<sup>1,\*</sup>

<sup>1</sup> Univ. Bordeaux, CNRS, CRPP, UMR 5031, 33600 Pessac, France

<sup>2</sup> LCMCP, Sorbonne Université, UMR 7574, 75005 Paris, France

<sup>3</sup> LCMD, CBI, ESPCI Paris, Université PSL, CNRS, 75005 Paris, France

<sup>4</sup> MIE, CBI, ESPCI Paris, Université PSL, CNRS, 75005 Paris, France

\* Correspondence: philippe.poulin@crpp.cnrs.fr

**Abstract:** Flowable electrodes, a versatile alternative to traditional solid electrodes for electrochemical applications, face challenges of high viscosity and carbon content, limiting flow and device performances. This study introduces colloidal suspensions of thin multiwall carbon nanotubes (MWCNTs) with diameters of 10-15 nm as electrode materials. These thin nanotubes, stabilized in water with surfactant, form percolated networks, exhibiting high conductivity (50 ms/cm) and stability at a low carbon content (below 2 wt%). Colloidal clustering is enhanced by weak depletion attractive interactions. The resulting suspensions display a yield stress and a shear thinning behavior with a low consistency index. They can easily flow at a nearly constant shear over a broad range of shear rates. They remain electrically conductive under shear making them promising for flow electrochemical applications. This work suggests that the use of depletion induced MWVNT aggregates addresses crucial issues in flow electrochemical applications, such as membrane fragility, operating energy, and pressure. These conductive colloidal suspensions offer thereby potential advancements in device performance and lifespan.

**Keywords:** carbon nanotubes; conductivity; flow electrochemistry, depletion

---

## 1. Introduction

Flowable electrodes are emerging as a versatile and promising alternative to traditional solid electrodes in various electrochemical applications, including flow capacitors [1-3] and water capacitive desalination [4-6]. Flow capacitors enjoy several promising features such as cost effectiveness and high energy storage capabilities. More critically, flow electrochemical technologies offer the possibility to decouple energy and power ratings. The energy scales with the volume of the reservoirs, whereas the charge transfer depends on the structure and stacks of the device. These features make flow capacitors and flow batteries particularly suited for storage of intermittent renewable energies. Flowable electrodes are also promising to address an environmental concern that is the global water resource shortage [7]. So-called flow capacitive deionization of water using carbon slurry was already introduced in 2013 [8], and has been the topic of extensive research since then [9-11]. Moreover, flow capacitive water desalination has been shown to be potentially more effective by implementing energy recovery during continuous deionization process [12].

In these applications, which are based on related physico-chemical mechanisms, carbon micro- or nano-particles [13] are suspended in an electrolyte medium, often containing formulating agents [14, 15]. At elevated concentrations, the colloidal particles create an electrically conductive network [16]. Upon application of a given voltage, ions from the volume of the electrolyte adsorb to the particle surface during the charging stage. Conversely, electrical charges are delivered to a current collector in the discharge mode. In contrast to their solid counterparts, flowable electrodes offer numerous ad-

48 vantages, such as a high surface area accessible from the entire electrolyte volume, en-  
49 hanced mass transport, and ease of replacement. Flowable electrodes in these applica-  
50 tions generally contain a high amount of carbon particles to ensure electrical conductiv-  
51 ity. High concentration yields viscoelastic suspensions, with a slurry like texture, im-  
52 peding easy flow. They necessitate high pressure and energy to be pumped. More criti-  
53 cally, a high concentration of carbon particles can result in plug formation or membrane  
54 rupture, limiting the performance and lifespan of devices [17]. This can become critical  
55 when using ion exchange membranes, which are costly components of energy storage or  
56 deionization devices.

57 To overcome these limitations, an approach consists of developing flowable elec-  
58 trodes with reduced carbon content. Reducing carbon content holds the potential for  
59 improving device stability, prolonging lifespan, and enhancing energetic efficiency. The  
60 first challenge towards this objective involves optimizing the rheological performance of  
61 carbon dispersions. Maintaining the dispersion's ability to flow is crucial. The second  
62 challenge is to formulate flowable dispersions that still exhibit sufficient electronic con-  
63 ductivity and electrochemical capacitance. Generally, as reviewed in references 3 and 18  
64 [3, 18], carbon-based slurries made of carbon black particles display conductivities below  
65 a few mS/cm, for carbon contents on the order of 10wt% or more. Moreover, the conduc-  
66 tivity of such slurries decreases sometimes substantially in flow conditions.

67 A way of maintaining conductivity over a wide shear rate range is to realize a fluid  
68 that can accommodate high shear rates with limited viscous dissipation. This is particu-  
69 larly the case of threshold fluids with low plastic viscosity or, more precisely, with a low  
70 consistency index and a high yield stress. Their equation of state is  $\sigma = \sigma_s + A\dot{\gamma}^n$ , where  
71  $A$  is the consistency index,  $\sigma_s$  the yield stress,  $\sigma$  the applied shear stress,  $\dot{\gamma}$  the shear  
72 rate and  $n$  the flow index [19]. In the limit of low  $A$ , the applied stress is maintained  
73 around the yield stress. The apparent viscosity, defined as  $\eta_{app} = \frac{\sigma}{\dot{\gamma}} = \frac{\sigma_s}{\dot{\gamma}} + A\dot{\gamma}^{n-1} \approx \frac{\sigma_s}{\dot{\gamma}}$ ,  
74 varies with the shear rate to the power -1. Flow in such fluids generally occurs through  
75 minute structural variations, characterized by fractures that continuously form and heal,  
76 especially as the fluid flows in close proximity to its yield stress. Such a behavior is usu-  
77 ally observed at low shear rates in yield stress fluids with high carbon contents [3, 20, 21].  
78 Realizing such flow conditions over a broad range of shear rates and at low carbon con-  
79 tents remains challenging.

80 Carbon nanotubes appear as natural candidates to meet the above challenges. In-  
81 deed, carbon nanotubes display a low percolation threshold at equilibrium because of  
82 their high aspect ratio,  $L/d$ , where  $d$  and  $L$  are the diameter and length of the nanotubes,  
83 respectively [22]. They hold therefore the potential for making conductive suspensions at  
84 low carbon content. Actually, such particles have been used as additives, mixed with  
85 other carbon particles, to improve capacitive water desalination performances [23-25].  
86 Nanotubes contribute to generate connectivity between the carbon particles. They have  
87 also been used as sole conductive species in aqueous electrodes with remarkable proper-  
88 ties [18, 26, 27]. In these earlier studies, electronic conductivities at equilibrium reached  
89 values between 5 to 10 ms/cm for carbon contents between 2.5 to 10 wt% typically. These  
90 remarkable properties result from the high conductivity of carbon nanotubes and from  
91 their high aspect ratio. Nevertheless, nanotubes used in these studies have a diameter of  
92 50-80 nm and a length of 10 $\mu$ m. Stabilization of such particles remains quite difficult be-  
93 cause of their large size and tendency to settle. In addition, the large size of the particles  
94 results in a more limited specific surface area and electrochemical capacitance compared  
95 to smaller colloidal nanoparticles.

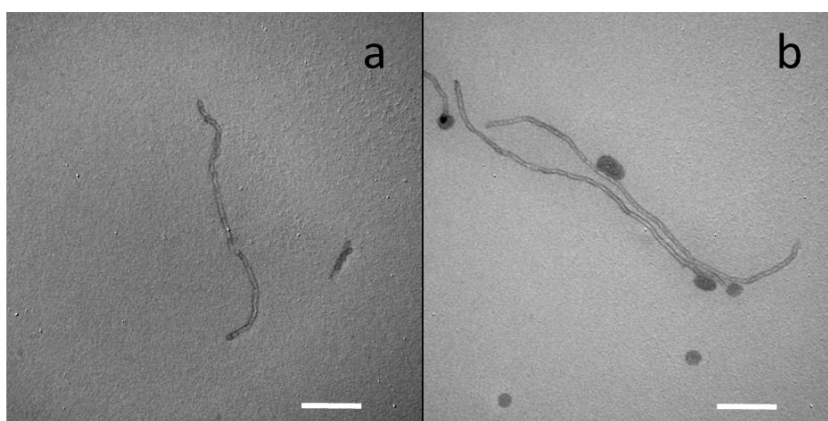
96 Following the investigation of carbon nanotube-based flowable electrodes, we re-  
97 port in the present work the realization of electrodes made of suspensions of thin multi-  
98 wall carbon nanotubes (MWCNTs) with a diameter of 10-15nm. These thinner nano-  
99 tubes do not settle, and can be more easily dispersed than large multiwall nanotubes. The  
100 nanotubes are stabilized in water with surfactant. Addition of excess surfactant is used to  
101 promote the formation of percolated networks in response to weak depletion attractive  
102 interactions [28]. These structures are shown to display high conductivity and high sta-

103 bility along with decent electrochemical capacitance. Typically, the best dispersions in-  
104 vestigated in the present work display an electronic conductivity of 50ms/cm for a carbon  
105 content below 2wt%. The viscosity of these suspensions does not exceed 2Pa.s for a shear  
106 rate of 5s<sup>-1</sup>. This original combination of high electronic conductivity and low plastic  
107 viscosity makes the present suspensions promising for flow electrochemical applications  
108 where membrane fragility, operating energy and pressure are key issues.  
109

## 110 2. Materials and methods

111 Two types of commercial Multiwall carbon nanotubes have been used, namely  
112 Graphistrength C100 materials from Arkema and NC 700 materials from Nanocyl. These  
113 nanotubes are produced by a chemical vapor deposition process and contain small frac-  
114 tions of metal catalysts. They are used as received without further purifications. Both  
115 materials have diameters in the 10-15nm range. Their length exceeds several microns  
116 in their raw state.

117 The carbon nanotubes are added to distilled water and stabilized with surfactant  
118 molecules. US4498 from US Research Nanomaterials is presently used. The exact molec-  
119 ular structure of the surfactant is unknown, but the compound is provided by US Re-  
120 search Nanomaterials as a non-ionic surfactant suited for the stabilization of carbon  
121 nanotubes in water. This surfactant contains aromatic groups with good affinity towards  
122 carbon nanotubes. Mother suspensions are prepared by mixing 1wt% of MWCNTs and  
123 2wt% of US4498 in distilled water for Arkema samples, and 0.5wt% of MWCNTs and  
124 2wt% of US4498 for Nanocyl samples. The suspensions are homogenized by tip soni-  
125 cation for 30 minutes. They are obtained using a Branson homogenizer, Sonifier model  
126 S-250A associated to a 13-mm step disruptor horn and a 3-mm tapered microtip, oper-  
127 ating at a 20-kHz frequency. The suspensions are found to be free of aggregates after such  
128 treatment. Tip sonication induces disentanglement and scission of the nanotubes [29, 30].  
129 The latter display a typical length in the range of 500nm-1 $\mu$ m. Transmission electron mi-  
130 crographs of isolated MWCNTs after sonication are shown in Figure 1.



131  
132 **Figure 1.** Transmission electron micrographs of individual Arkema (a) and Nanocyl (b) MWCNT  
133 after sonication. Scale 100nm.

134 The mother suspensions are then further concentrated by dialysis. This is realized by  
135 placing the suspensions in Spectra/Por dialysis membrane bags with a 6-8 kD molecular  
136 weight cut-off. This cut-off allows the transport of water and surfactant molecules, but  
137 the membranes retain MWCNTs. The dialysis bags are placed in contact with a Spec-  
138 tra/gel absorbing hydrogel. Water and surfactant molecules are adsorbed by the gel, and  
139 the concentration of MWCNTs in the dialysis bag increases with time. The concentration  
140 of surfactant also increases nearly similarly because of its much lower diffusion com-  
141 pared to that of water molecules. Using aqueous solutions of surfactant, we have actually  
142 verified that the transport of surfactant across the membrane is negligible on the time  
143 scale of the present experiments. Typically, the surfactant concentration is found to in-

144 crease almost linearly with the reduction of volume of the solution. The ratio of surfac-  
145 tant to MWCNTs can therefore be considered as constant when the total concentration of  
146 dried materials increases. Varying the time of dialysis allows different concentrations of  
147 MWCNTs to be achieved. The amount of dried materials, including surfactant and  
148 MWCNTs, contained in the suspensions is measured by dry extract experiments. The  
149 weight fraction of MWCNTs is deduced from the known initial ratio of surfactant to  
150 MWCNT. The most concentrated samples investigated in the present work have a  
151 MWCNT weight fraction above 4wt% obtained after 6 hours of dialysis.

152 The phase behavior of the samples is assessed by optical microscopy using a Leica  
153 DM2500 microscope.

154 Conductivity of the samples at equilibrium is measured using a Radiometer CDC749  
155 conductivity cell connected to a Keithley 2000 multimeter. A constant voltage of 0.5V is  
156 applied between the electrodes of the cell, and the current is measured as a function of  
157 time. The current decreases until it reaches a stationary value, typically after a few  
158 minutes. The stationary current corresponds to the contribution of electronic conductivity  
159 of the samples, without the contribution of ionic conductivity [31].

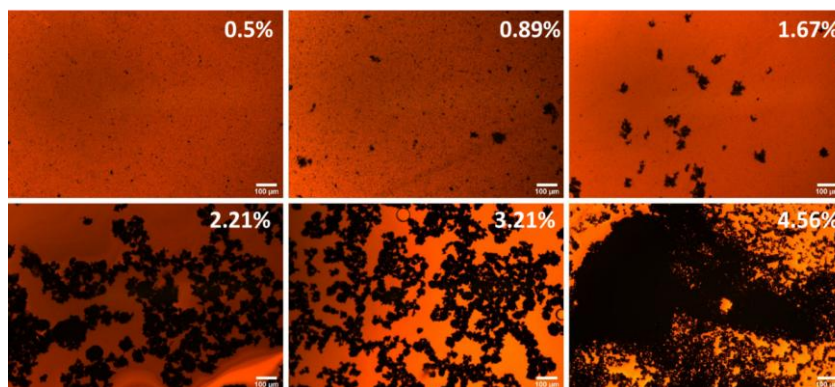
160 Conductivity in shear flow is measured using a Couette cell (Caplim Rheophysique  
161 West 3400) as detailed in [3]. In the present work, conductivity is measured in the radial  
162 direction of the Couette cell with two concentric circular electrodes. The conductivity  
163 corresponds to the conduction in the shear plane, perpendicular to the flow direction.

164 The rheological properties are characterized by an AR1000 controlled stress  
165 rheometer from TA Instrument. A ramp of shear rate is applied from  $200\text{ s}^{-1}$  to  $0.1\text{ s}^{-1}$ , with  
166 5 points per decade. Each shear rate is maintained during 30 seconds and the viscosity is  
167 measured by averaging the measurements over the last 5 seconds. The temperature is set  
168 with a Peltier system at  $20^\circ\text{ C}$ .

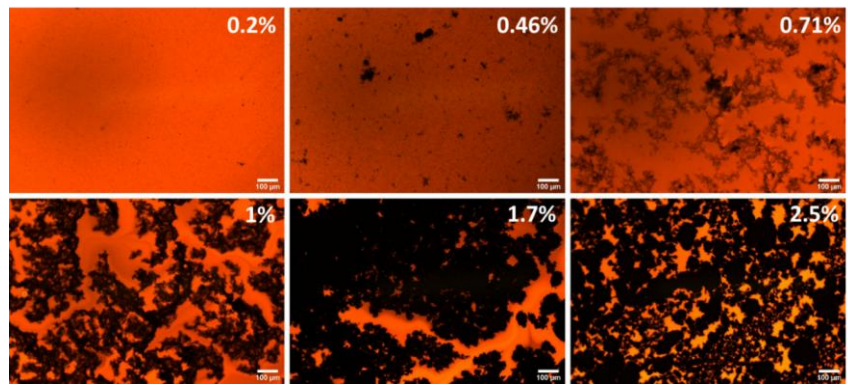
169 The electrochemical capacitance of the suspensions is measured in a two-electrodes  
170 symmetric cell configuration. The setup is described in detail in [3]. The liquid electrodes  
171 have the same volume and are separated from each other by using an anion exchange  
172 membrane (SnakeSkin®Dialysis Tubing 1000 MWCO). Cyclic voltammetry is performed  
173 using an Autolab PGSTAT204 Metrohm potentiostat/galvanostat.

### 174 3. Results and discussion

175 Optical micrographs of MWCNTs suspensions are shown in Figure 2 for Arkema  
176 samples and in Figure 3 for Nanocyl samples. It is observed in both cases that aggregates  
177 tend to form with increasing the concentration of MWCNTs and surfactant in the sus-  
178 pensions. This aggregation behavior is ascribed to depletion attraction between the  
179 nanotubes due to the presence of surfactant micelles [28, 32]. Depletion attraction is weak  
180 [33], and results in loose aggregates that do not settle with time. The aggregates remain in  
181 constant equilibrium with dispersed and individualized nanotubes.  
182

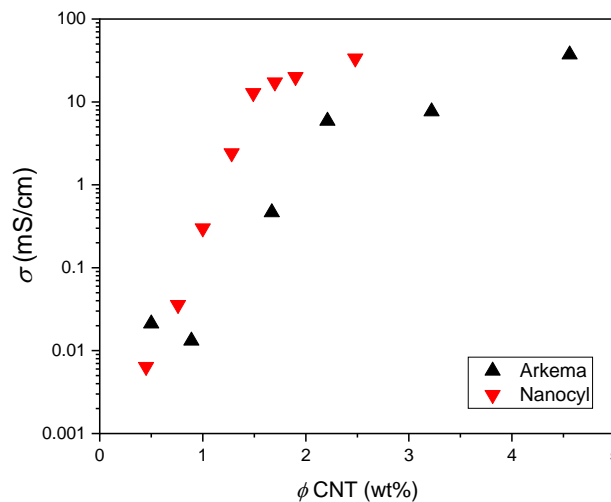


183  
184 **Figure 2.** Optical micrographs of aqueous suspensions of Arkema nanotubes at different weight  
185 fractions. Large aggregates form in response to the depletion attractive interactions. Scale 100 nm.



186  
187  
188 **Figure 3.** Optical micrographs of aqueous suspensions of Nanocyl nanotubes at different weight fractions. Large aggregates form in response to the depletion attractive interactions. Scale 100nm.

189  
190  
191  
192  
193  
194  
195  
196  
197  
198 The results of electronic conductivity measurements at equilibrium are shown in Figure 4. A typical percolation type behavior is observed. The conductivity increases by several orders of magnitude at the percolation threshold. These thresholds are about 1 and 1.5 wt% for Nanocyl and Arkema materials, respectively. Particularly high conductivity values are obtained for concentrations above 2 wt% for both materials, approaching 100ms/cm. Note that the small difference in percolation thresholds observed for Nanocyl and Arkema materials can be explained by the slightly greater aspect ratio of Nanocyl materials compared to Arkema systems. This is consistent with optical microscope images reported in Fig. 2 and 3 where Nanocyl tend to form a sample-spanning network of aggregates at a lower weight fraction.



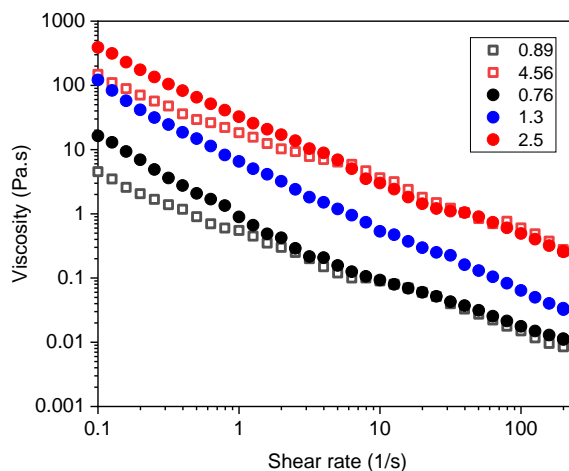
199  
200  
201 **Figure 4.** Electronic conductivity of Arkema and Nanocyl suspensions as a function of concentrations of nanotubes (%wt).

202  
203  
204  
205  
206  
207  
208  
209  
210 Rheological properties of samples with different weight fractions are shown in Figure 5. The presence of MWCNTs results in a clear shear thinning behavior of the suspensions. The viscosity decreases as a function of shear rate by three orders of magnitude, with an exponent close to -1, revealing thereby a yield stress fluid behavior. A distinctive feature of these suspensions is their low carbon content and very low consistency index, ensuring that the stress remains near a constant value across a broad range of shear rate. A likely representation of the flow involves the formation of a small number of weak regions that are the locus of rearrangements-fractures that constantly form and heal.

211  
212 This behavior results in interesting effective viscosity properties. The suspensions containing 1.8wt% of Nanocyl material, which are highly conductive, display an effective

213  
214  
215  
216

viscosity of 1.2 Pa.s for a shear rate of 5 s<sup>-1</sup>. Even highly concentrated Arkema suspensions with 4.5 wt% of MWCNT still display a limited viscosity of only 6.4 Pa.s at a shear rate of 5 s<sup>-1</sup>. The present results therefore confirm that the use of thin MWCNTs enables the realization of highly conductive suspensions with reasonably low apparent viscosity.

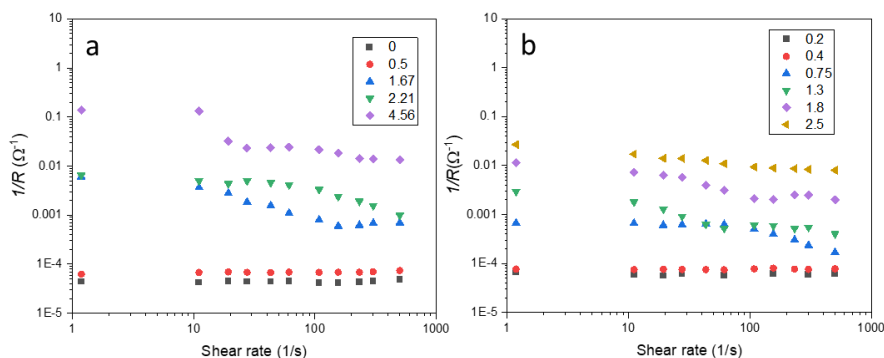


217  
218  
219

**Figure 5.** Viscosity as a function of shear rate for suspensions of Arkema (open squares) and Nanocyl (filled circles) MWCNT. Weight fractions of the samples are indicated in wt% in inset.

220  
221  
222  
223  
224  
225  
226  
227  
228  
229  
230  
231

In order to confirm the potential interest of the present suspensions for flow electrochemical applications, it remains critical to check their conductivity under shear. Results of conductance measurements in a Couette cell [3] are shown in Figure 6 for Arkema and Nanocyl materials. The conductance,  $1/R$ , is plotted as a function of shear rate, where  $R$  is the resistance measured between the concentric circular electrodes. It is observed that the conductance decreases very slightly for all the investigated MWCNT suspensions. This slight decrease can result from small fractures that allows flow of the material. The fact that conductivity does not vanish with shear shows that the structural changes in nanotube suspensions remain limited. This is consistent with the description given above of a yield stress fluid with a low consistency index. The material resist against fluidization and disruption of conductive pathways up to shear rates of several hundreds of s<sup>-1</sup>, even for solid contents as low as 1 wt%.



232  
233  
234

**Figure 6.** Conductance of aqueous suspensions of Arkema (a) and Nanocyl (b) MWCNTs as a function of shear rate. Weight fractions of the samples are indicated in wt% in inset.

235  
236  
237  
238  
239

Results of cyclic voltammetry experiments [34] are shown in Figure 7. The current  $I$  was measured when the voltage  $V$  was varied from -0.5V to 0.5V at a scan rate ( $\frac{dV}{dt}$ ) of 50mV/s. The specific gravimetric capacitance  $C_{sp}$  is then deduced by normalizing the current measured for  $V=0$  by the weight  $m$  of carbon material contained in the volume of the cell. The cell volume in the present setup is 0.24 cm<sup>3</sup> per electrode [3].

$$C_{sp} = \frac{2I}{m \cdot \left(\frac{dV}{dt}\right)}$$

The Arkema suspension containing 4.5wt% of MWCNT, and the Nanocyl suspension containing 1.8wt% of MWCNT respectively display specific gravimetric capacitance of 2F/g and 6.5F/g. These values are not particularly high but comparable to those measured for low viscosity carbon black suspensions at similar scan rates [3].

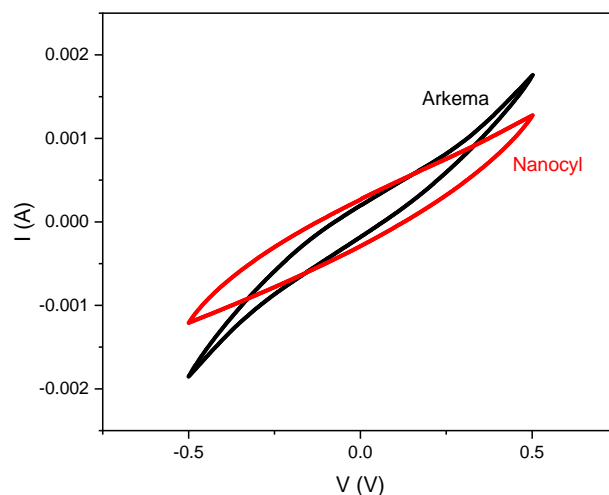


**Figure 7.** Cyclic voltammetry of suspensions containing 4.5 wt% of Arkema MWCNT and 1.8 wt% of Nanocyl MWCNTs.

## 5. Conclusion

In conclusion, this study presents a novel approach to address challenges associated with flowable electrodes in electrochemical applications by introducing colloidal suspensions of thin multiwall carbon nanotubes (MWCNTs). The suspensions are stabilized in water with a non-ionic surfactant, and are further concentrated through a dialysis process. The used surfactant molecules contain aromatic groups that promote their adsorption at the interface of the nanotubes. The suspensions are homogenized by tip sonication prior concentration by dialysis. Characterizations of electrical properties demonstrate a percolation-type behavior in electronic conductivity with a strong increase above a critical concentration of carbon nanotubes. Additionally, the suspensions display a shear-thinning behavior in rheological properties, and a stable conductance under shear conditions. Clustering of nanotubes is enhanced and conductivity improved because of weak depletion attractive interactions between the nanotubes. The depletion attraction is attributed to the presence of a large excess of surfactant micelles. Shear induces small structural variations of the depletion-induced aggregates through constant minute structural rearrangements. These reversible rearrangements allow maintaining flow at a nearly constant stress of a globally persistent percolated and conductive network. Optimal suspensions display high conductivity on the order of 50 ms/cm at a low carbon content, below 2 wt%. Cyclic voltammetry experiments reveal specific gravimetric capacitance values comparable to low viscosity carbon black suspensions. This work contributes therefore to advancing the field of flowable electrodes, offering a potential solution to the challenges associated with high viscosity and carbon content. The use of thin MWCNTs in colloidal suspensions presents a promising approach for further developments in flow electrochemical applications, emphasizing the importance of balancing electronic conductivity and viscosity for improved device performance and longevity. Future research directions should focus on enhancing energy storage capabilities. At present, using a low carbon content is naturally an intrinsic limitation for achieving high gravimetric capacitance. This limitation can be somehow mitigated using thin carbon nanotubes, but still remains



276 an obstacle. A promising perspective would consist in using pseudo-capacitive flow  
277 electrodes by introducing red-ox active species, such as quinone derivatives, in the for-  
278 mulations. This approach has already been proved to be efficient at increasing perfor-  
279 mances of flow electrochemical systems [35-39].

280  
281  
282 **Author Contributions:**

283 Conceptualization, A.C., N.B. and P.P.; methodology, N.B., W.N., P.P.; formal analysis, N.B., A.C.,  
284 J.Y. and P.P.; investigation, M.H., W.N. and X.B.; resources, W.N. and X.B.; writing—original draft  
285 preparation, M.H. and P.P.; writing—review and editing, N.B., A.C., J.Y. and P.P.; supervision,  
286 N.B., W.N. and P.P.; funding acquisition, N.B., A.C. and P.P.. All authors have read and agreed to  
287 the published version of the manuscript.

288 **Funding:** This work was supported by a public grant overseen by the French National Research  
289 Agency (ANR), Project Reference No. ANR19-CE06-0026 (ElectroFluid).

290 **Data Availability Statement**

291 The data that support the findings of this study are available from the corresponding author upon  
292 reasonable request.

293 **Conflicts of Interest:** “The authors declare no conflicts of interest.”  
294

295 **References**

- 296 1- Presser, V.; Dennison, C. R.; Campos, J.; Knehr, K. W.; Kumbur, E. C.; Gogotsi, Y. The Electrochemical Flow Capacitor: A New  
297 Concept for Rapid Energy Storage and Recovery. *Advanced Energy Materials* **2012**, *2* (7), 895-902. DOI: 10.1002/aenm.201100768.
- 298 2- Campos, J. W.; Beidaghi, M.; Hatzell, K. B.; Dennison, C. R.; Musci, B.; Presser, V.; Kumbur, E. C.; Gogotsi, Y. Investigation of  
299 carbon materials for use as a flowable electrode in electrochemical flow capacitors. *Electrochimica Acta* **2013**, *98*, 123-130. DOI:  
300 10.1016/j.electacta.2013.03.037.
- 301 3- Alfonso, M. S.; Parant, H.; Yuan, J. K.; Neri, W.; Laurichesse, E.; Kampioti, K.; Colin, A.; Poulin, P. Highly conductive colloidal  
302 carbon based suspension for flow-assisted electrochemical systems. *Isience* **2021**, *24* (5). DOI: 10.1016/j.isci.2021.102456.
- 303 4- Yu, F.; Yang, Z. Q.; Cheng, Y. J.; Xing, S. Y.; Wang, Y. Y.; Ma, J. A comprehensive review on flow-electrode capacitive deionization:  
304 Design, active material and environmental application. *Separation and Purification Technology* **2022**, *281*. DOI:  
305 10.1016/j.seppur.2021.119870.
- 306 5- Ma, J. J.; Zhang, C. Y.; Yang, F.; Zhang, X. D.; Suss, M. E.; Huang, X.; Liang, P. Carbon Black Flow Electrode Enhanced Electro-  
307 chemical Desalination Using Single-Cycle Operation. *Environmental Science & Technology* **2020**, *54* (2), 1177-1185. DOI:  
308 10.1021/acs.est.9b04823.
- 309 6- Zhang, C. Y.; Ma, J. X.; Wu, L.; Sun, J. Y.; Wang, L.; Li, T. Y.; Waite, T. D. Flow Electrode Capacitive Deionization (FCDI): Recent  
310 Developments, Environmental Applications, and Future Perspectives. *Environmental Science & Technology* **2021**, *55* (8), 4243-4267.  
311 DOI: 10.1021/acs.est.0c06552.
- 312 7- Yang, F.; He, Y. F.; Rosentsvit, L.; Suss, M. E.; Zhang, X. R.; Gao, T.; Liang, P. Flow-electrode capacitive deionization: A review and  
313 new perspectives. *Water Research* **2021**, *200*. DOI: 10.1016/j.watres.2021.117222.
- 314 8- Jeon, S. I.; Park, H. R.; Yeo, J. G.; Yang, S.; Cho, C. H.; Han, M. H.; Kim, D. K. Desalination via a new membrane capacitive de-  
315 ionization process utilizing flow-electrodes. *Energy & Environmental Science* **2013**, *6* (5), 1471-1475. DOI: 10.1039/c3ee24443a.
- 316 9- Doornbusch, G. J.; Dykstra, J. E.; Biesheuvel, P. M.; Suss, M. E. Fluidized bed electrodes with high carbon loading for water de-  
317 salination by capacitive deionization. *Journal of Materials Chemistry A* **2016**, *4* (10), 3642-3647. DOI: 10.1039/c5ta10316a.
- 318 10- Yang, S.; Park, H. R.; Yoo, J.; Kim, H.; Choi, J.; Han, M. H.; Kim, D. K. Plate-Shaped Graphite for Improved Performance of  
319 Flow-Electrode Capacitive Deionization. *Journal of the Electrochemical Society* **2017**, *164* (13), E480-E488. DOI: 10.1149/2.1551713jes.
- 320 11- Tang, K. X.; Yiaccoumi, S.; Li, Y. P.; Tsouris, C. Enhanced Water Desalination by Increasing the Electroconductivity of Carbon  
321 Powders for High-Performance Flow-Electrode Capacitive Deionization. *Acs Sustainable Chemistry & Engineering* **2019**, *7* (1),  
322 1085-1094. DOI: 10.1021/acssuschemeng.8b04746.
- 323 12- Rommerskirchen, A.; Linnartz, C. J.; Müller, D.; Willenberg, L. K.; Wessling, M. Energy Recovery and Process Design in Con-  
324 tinuous Flow Electrode Capacitive Deionization Processes. *Acs Sustainable Chemistry & Engineering* **2018**, *6* (10), 13007-13015. DOI:  
325 10.1021/acssuschemeng.8b02466.
- 326 13- Campos, J. W.; Beidaghi, M.; Hatzell, K. B.; Dennison, C. R.; Musci, B.; Presser, V.; Kumbur, E. C.; Gogotsi, Y. Investigation of  
327 carbon materials for use as a flowable electrode in electrochemical flow capacitors. *Electrochimica Acta* **2013**, *98*, 123-130. DOI:  
328 10.1016/j.electacta.2013.03.037.
- 329 14- Lee, J. H.; Weingarh, D.; Grobelsek, I.; Presser, V. Use of Surfactants for Continuous Operation of Aqueous Electrochemical Flow  
330 Capacitors. *Energy Technology* **2016**, *4* (1), 75-84. DOI: 10.1002/ente.201500243.
- 331 15- Torop, J.; Summer, F.; Zadin, V.; Koironen, T.; Jänes, A.; Lust, E.; Aabloo, A. Low concentrated carbonaceous suspensions as-  
332 sisted with carboxymethyl cellulose as electrode for electrochemical flow capacitor. *European Physical Journal E* **2019**, *42* (1). DOI:  
333 10.1140/epje/i2019-11766-2.
- 334 16- Akuzum, B.; Singh, P.; Eichfeld, D. A.; Agartan, L.; Uzun, S.; Gogotsi, Y.; Kumbur, E. C. Percolation Characteristics of Conduc-  
335 tive Additives for Capacitive Flowable (Semi-Solid) Electrodes. *Acs Applied Materials & Interfaces* **2020**, *12* (5), 5866-5875. DOI:  
336 10.1021/acsaami.9b19739.

- 338 17- Tang, K. X.; Yiacoumi, S.; Li, Y. P.; Tsouris, C. Enhanced Water Desalination by Increasing the Electroconductivity of Carbon  
339 Powders for High-Performance Flow-Electrode Capacitive Deionization. *Acs Sustainable Chemistry & Engineering* **2019**, *7* (1),  
340 1085-1094. DOI: 10.1021/acssuschemeng.8b04746.
- 341 18- Gloukhovski, R.; Suss, M. E. Measurements of the Electric Conductivity of MWCNT Suspension Electrodes with Varying Potas-  
342 sium Bromide Electrolyte Ionic Strength. *Journal of the Electrochemical Society* **2020**, *167* (2). DOI: 10.1149/1945-7111/ab6a88.
- 343 19- Balmforth, N. J.; Frigaard, I. A.; Ovarlez, G. Yielding to Stress: Recent Developments in Viscoplastic Fluid Mechanics. *Annual*  
344 *Review of Fluid Mechanics, Vol 46* **2014**, *46*, 121-146. DOI: 10.1146/annurev-fluid-010313-141424.
- 345 20- Ouyang, L. X.; Wu, Z. H.; Wang, J.; Qi, X. P.; Li, Q.; Wang, J. T.; Lu, S. G. The effect of solid content on the rheological properties  
346 and microstructures of a Li-ion battery cathode slurry. *Rsc Advances* **2020**, *10* (33), 19360-19370. DOI: 10.1039/d0ra02651d.
- 347 21- Larsen, T.; Royer, J.R.; Laidlaw, F.H.J.; Poon, W.C.K.; Larsen, T.; Andreasen, S.J.; Christiansen, J.C. Controlling the rheo-electric  
348 properties of graphite/carbon black suspensions by 'flow switching'. arXiv:2311.05302 [cond-mat.soft], DOI:  
349 10.48550/arXiv.2311.05302
- 350 22- Balberg, I.; Anderson, C. H.; Alexander, S.; Wagner, N. EXCLUDED VOLUME AND ITS RELATION TO THE ONSET OF  
351 PERCOLATION. *Physical Review B* **1984**, *30* (7), 3933-3943. DOI: 10.1103/PhysRevB.30.3933.
- 352 23- Cho, Y.; Yoo, C. Y.; Lee, S. W.; Yoon, H.; Lee, K. S.; Yang, S.; Kim, D. K. Flow-electrode capacitive deionization with highly en-  
353 hanced salt removal performance utilizing high-aspect ratio functionalized carbon nanotubes. *Water Research* **2019**, *151*, 252-259.  
354 DOI: 10.1016/j.watres.2018.11.080.
- 355 24- Chen, K. Y.; Shen, Y. Y.; Wang, D. M.; Hou, C. H. Carbon nanotubes/activated carbon hybrid as a high-performance suspension  
356 electrode for the electrochemical desalination of wastewater. *Desalination* **2022**, *522*. DOI: 10.1016/j.desal.2021.115440.
- 357 25- Wang, Z. L.; Hu, Y. D.; Wei, Q.; Li, W. S.; Liu, X.; Chen, F. M. Enhanced Desalination Performance of a Flow-Electrode Capacitive  
358 Deionization System by Adding Vanadium Redox Couples and Carbon Nanotubes. *Journal of Physical Chemistry C* **2021**, *125* (2),  
359 1234-1239. DOI: 10.1021/acs.jpcc.0c09058.
- 360 26- Petek, T. J.; Hoyt, N. C.; Savinell, R. F.; Wainright, J. S. Characterizing Slurry Electrodes Using Electrochemical Impedance  
361 Spectroscopy. *Journal of the Electrochemical Society* **2016**, *163* (1), A5001-A5009. DOI: 10.1149/2.0011601jes.
- 362 27- Cohen, H.; Eli, S. E.; Jogi, M.; Suss, M. E. Suspension Electrodes Combining Slurries and Upflow Fluidized Beds. *Chemsuschem*  
363 **2016**, *9* (21), 3045-3048. DOI: 10.1002/cssc.201601008.
- 364 28- Vigolo, B.; Coulon, C.; Maugey, M.; Zakri, C.; Poulin, P. An experimental approach to the percolation of sticky nanotubes. *Science*  
365 **2005**, *309* (5736), 920-923. DOI: 10.1126/science.1112835.
- 366 29- Lucas, A.; Zakri, C.; Maugey, M.; Pasquali, M.; van der Schoot, P.; Poulin, P. Kinetics of Nanotube and Microfiber Scission under  
367 Sonication. *Journal of Physical Chemistry C* **2009**, *113* (48), 20599-20605. DOI: 10.1021/jp906296y.
- 368 30- Pagani, G.; Green, M. J.; Poulin, P.; Pasquali, M. Competing mechanisms and scaling laws for carbon nanotube scission by  
369 ultrasonication. *Proceedings of the National Academy of Sciences of the United States of America* **2012**, *109* (29), 11599-11604. DOI:  
370 10.1073/pnas.1200013109.
- 371 31- Parant, H.; Muller, G.; Le Mercier, T.; Tarascon, J. M.; Poulin, P.; Colin, A. Flowing suspensions of carbon black with high elec-  
372 tronic conductivity for flow applications: Comparison between carbons black and exhibition of specific aggregation of carbon par-  
373 ticles. *Carbon* **2017**, *119*, 10-20. DOI: 10.1016/j.carbon.2017.04.014.
- 374 32- Kyrylyuk, A. V.; van der Schoot, P. Continuum percolation of carbon nanotubes in polymeric and colloidal media. *Proceedings of*  
375 *the National Academy of Sciences of the United States of America* **2008**, *105* (24), 8221-8226. DOI: 10.1073/pnas.0711449105.
- 376 33- Mao, Y.; Cates, M. E.; Lekkerkerker, H. N. W. Depletion force in colloidal systems. *Physica A* **1995**, *222* (1-4), 10-24. DOI:  
377 10.1016/0378-4371(95)00206-5.
- 378 34- Electrochemical Methods: Fundamentals and Applications, 2nd Edition, Allen J. Bard, Larry R. Faulkner. December 2000 Wiley  
379 Ed. ISBN: 978-0-471-04372-0

380 35- Hatzell, K. B.; Beidaghi, M.; Campos, J. W.; Dennison, C. R.; Kumbur, E. C.; Gogotsi, Y. A high performance pseudocapacitive  
381 suspension electrode for the electrochemical flow capacitor. *Electrochimica Acta* **2013**, *111*, 888-897. DOI:  
382 10.1016/j.electacta.2013.08.095.

383 36- Hou, S. J.; Wang, M.; Xu, X. T.; Li, Y. D.; Li, Y. J.; Lu, T.; Pan, L. K. Nitrogen-doped carbon spheres: A new high-energy-density  
384 and long life pseudo-capacitive electrode material for electrochemical flow capacitor. *Journal of Colloid and Interface Science* **2017**, *491*,  
385 161-166. DOI: 10.1016/j.jcis.2016.12.033.

386 37- Hunt, C.; Mattejat, M.; Anderson, C.; Sepunaru, L.; Ménard, G. Symmetric Phthalocyanine Charge Carrier for Dual Redox Flow  
387 Battery/Capacitor Applications. *Acs Applied Energy Materials* **2019**, *2* (8), 5391-5396. DOI: 10.1021/acsaem.9b01317.

388 38- Tomai, T.; Saito, H.; Honma, I. High-energy-density electrochemical flow capacitors containing quinone derivatives impreg-  
389 nated in nanoporous carbon beads. *Journal of Materials Chemistry A* **2017**, *5* (5), 2188-2194. DOI: 10.1039/c6ta08733g.

390 39- Yoon, H.; Kim, H. J.; Yoo, J. J.; Yoo, C. Y.; Park, J. H.; Lee, Y. A.; Cho, W. K.; Han, Y. K.; Kim, D. H. Pseudocapacitive slurry  
391 electrodes using redox-active quinone for high-performance flow capacitors: an atomic-level understanding of pore texture and  
392 capacitance enhancement. *Journal of Materials Chemistry A* **2015**, *3* (46), 23323-23332. DOI: 10.1039/c5ta05403f.

393

394 **Disclaimer/Publisher's Note:** The statements, opinions and data contained in all publications are solely those of the individual  
395 author(s) and contributor(s) and not of MDPI and/or the editor(s). MDPI and/or the editor(s) disclaim responsibility for any injury  
396 to people or property resulting from any ideas, methods, instructions or products referred to in the content.